# Evidence of half-metallic interface magnetism via local moment formation in Co based Heusler alloys

N. D. Telling[1], P. S. Keatley[2], G. van der Laan[1], R. J. Hicken[2], E. Arenholz[3], Y. Sakuraba[4], M. Oogane[4], Y. Ando[4] and T. Miyazaki[4]

[1]*Magnetic Spectroscopy Group, CCLRC Daresbury Laboratory, Warrington WA4 4AD, United Kingdom*

[2]*School of Physics, University of Exeter, Stocker Road, Exeter EX4 4QL, United Kingdom*

[3]*Advanced Light Source, Lawrence Berkeley National Laboratory, Berkeley, California 94720, USA*

[4]*Department of Applied Physics, Graduate School of Engineering, Tohoku University, Aoba-yama 6-6-05, Sendai 980-8579, Japan*

In this work we use a combination of x-ray magnetic circular and linear dichroism (XMCD and XMLD) techniques to examine the formation of local moments in Heusler alloys of the composition $Co_2MnX$ (where X=Si or Al). The existence of local moments in a half-metallic system is reliant upon the band gap in the minority-spin states. By utilising the element-specific nature of x-ray techniques we are able to explore the origin of the minority-spin band gap in the partial density of states (PDOS), via the degree of localisation of moments on Co and Mn atoms. We observe a crucial difference in the localisation of the Co moment when comparing $Co_2MnSi$ (CMS) and $Co_2MnAl$ (CMA) films that is consistent with the predicted larger minority-spin gap in the Co PDOS for CMS. These results provide important evidence for the dominant role of the Co minority-spin states in realising half-metallic ferromagnetism (HMF) in these Heusler alloys. They also demonstrate a direct method for measuring the degree of interfacial HMF in the raw materials without the need for fabricating spin-transport devices.

PACS number(s): 75.70.-i, 78.70.Dm, 72.25.-b, 75.47.-m

## I. INTRODUCTION

Half-metallic ferromagnetism (HMF) is observed in materials where the majority-spin states have metallic character whilst the minority-spin band contains an energy gap at the Fermi level [1]. This unique property leads to 100% spin-polarization and thus makes the materials extremely attractive candidates for spintronic applications. A great deal of theoretical effort has been applied to understand the origin of band gaps in half-metallic ferromagnets such as the full Heusler alloys $Co_2MnZ$ (where Z=Si, Al, Ge, Sn or Ga). The band gap in the minority-spin states is thought to arise from the hybridisation of Co and Mn *d* orbitals [2-4]. The overall gap is determined by the Co-Co interaction while the 'effective' gap in the Mn partial density of states (PDOS) is much larger as a result of the Co-Co-Mn hybridisation. Typically, experimental results on these materials provide indirect evidence for half-metallic ferromagnetism (HMF) through the observation of large tunnelling magnetoresistance (TMR) [5-7]. Thus a systematic study of the band gap in the PDOS for the different elements in these alloys is asked for. Although surface science techniques, such as spin resolved photoemission, can directly probe the spin-polarisation at a half-metal surface, they cannot be used to access the crucial interface region of half-metal and barrier layer (typically alumina or MgO) which is responsible for the TMR.

Kübler *et al.* [8] pointed out that a local exclusion of minority spin around atoms in Heusler alloys leads to the formation of so-called 'ideal' local moments. The existence of these local moments in a half-metallic system is reliant upon the band gap in the minority-spin states. Put another way, an experimental observation of local moments is thus crucial evidence of the minority-spin gap and hence HMF in the material. X-ray magnetic dichroism techniques could be a powerful tool for studying such systems as they are sensitive to the localisation of magnetic moments in an element-specific way. Previously it has been shown that the existence of local moments gives rise to a multiplet fine structure in the x-ray magnetic circular dichroism (XMCD) spectra [9,10]. In addition, the x-ray magnetic linear dichroism (XMLD) effect is found to be several times larger in a local moment system than in a purely itinerant one [11,12].

In this work we performed both XMCD and XMLD measurements on Heusler alloys of the form $Co_2MnSi$ (CMS) and $Co_2Al$ (CMA). By utilising the element-specific nature of the techniques we were able to separately explore the degree of localisation of moments on Co and Mn atoms in the alloy. Differences in the degree of localisation of the moments in CMS and CMA films are discussed with respect to calculations of the PDOS in these two systems. We show that the Co moment has more itinerant character in the CMA sample than in the CMS film, suggesting a smaller gap in the Co minority-spin band for CMA. These results are consistent with the measured weaker spin-polarisation in the CMA films compared to CMS [6]. This demonstrates the predicted dominant role of the Co-Co interaction on the overall minority-spin gap and hence HMF.

## II. EXPERIMENTAL

Epitaxial (100) orientated CMS and CMA layers were prepared on Cr-buffered MgO(100) substrates at ambient temperature using inductively coupled plasma (ICP) assisted magnetron sputtering. A composition-adjusted sputtering target (43.7% Co, 27.95% Mn, 28.35% Si) was used to achieve stoichiometric CMS films, whilst a stoichiometric Co–Mn–Al (Co: 50.0%, Mn: 25.0%, Al: 25.0%) composition target was used for the CMA films. The alloy layers were subsequently *in-situ* annealed in order to provide optimum site ordering with either the $L2_1$ structure (CMS films) or B2 structure (CMA films). Following annealing, a 1.3 nm Al capping layer was deposited to prevent oxidation. The crystal structure of the prepared Heusler alloy thin films was verified by x-ray diffraction with in-plane and out-of-plane geometries. Full details of the sample preparation and characterisation can be found elsewhere [6].

X-ray absorption (XA) spectroscopy and XMCD measurements were performed at the Advanced Light Source on beamlines 6.3.1 and 4.0.2 using circularly polarised soft x-rays. The XA spectra were collected using the total electron yield (TEY) method of detection. The sample was inclined at an angle of 30° to the x-ray beam and the data collected at fixed photon helicity by reversing a magnetic field of 500 Oe along the x-ray beam, for each photon energy point in the scan (Fig. 1(a)).

The XMLD measurements were obtained on beamline 4.0.2 using an 8-pole electromagnet [13]. The XA was again measured in TEY with the sample aligned with

the x-ray polarisation vector along the in-plane [100] film axis as shown in Fig. 1(b). At each point in the scan the magnetic field was applied parallel and then orthogonal to the polarisation vector. In order to improve the electron yield signal, the magnetic field was canted slightly out of the sample surface. However, this does not affect the XMLD measurement as the surface normal represents a hard magnetic axis in these samples. The measurement was then repeated with the polarisation vector rotated by 90º to lie along the [010] sample axis. As the Heusler films studied here have a cubic structure, the XMLD obtained by rotation of either the x-ray polarisation vector, or the magnetisation direction, are simple inversions of each other [12]. Thus the final XMLD spectrum was obtained by subtracting these two curves in order to remove any non-dichroic artefacts. The sample was then rotated by 45º so that the polarisation vector was parallel to the [110] or [1-10] axes, as shown in Fig. 1(c), and the XMLD obtained as before.

## III. RESULTS AND DISCUSSION

The XMCD measured across the Co $L_{2,3}$ absorption edge for the CMS and CMA film is shown in Fig. 2(a), together with that obtained from a Co reference film capped with Al. The multiplet fine structure in the CMS film can be clearly seen and is similar to that observed previously in this material [14,15]. The observation of this fine structure is indicative of a degree of localised character to the Co moment and arises from intra-atomic exchange and electron correlation effects. In contrast, the spectrum obtained from the CMA film more closely resembles the Co/Al reference film. The corresponding XMCD spectra measured around the Mn $L_{2,3}$ are shown in Fig. 2(b). Again a clear multiplet fine structure can be seen in the XMCD from the CMS film and is similar to spectra obtained from a range of Heusler alloys containing Mn [14-18]. However, unlike the Co XMCD there is evidence of multiplet structure in the Mn XMCD from the CMA film (note the feature at the $L_2$ absorption edge), although of weaker intensity than for the CMS film.

These results suggest that whilst the Co moment has more itinerant character in the CMA film, the Mn moment has a degree of localisation for both materials. The reason for this difference can be understood by considering the partial density of states (PDOS). For CMS films, the Fermi level lies in the middle of the overall minority-spin

gap such that there is an absence of minority-spin DOS for both Co and Mn atoms [6]. Hence the exclusion of minority-spin should occur around both Co and Mn atoms leading to local moment formation on both sites, in agreement with the XMCD from this film. The calculated PDOS for the CMA film in the B2 structure is shown in Fig. 3 [6]. In this case the Fermi level is positioned close to the edge of the overall gap. As the Co band gap is narrower than the Mn gap, this leads to a finite minority-spin Co DOS at the Fermi level, as seen in the inset to Fig. 3. The Mn minority-spin DOS is close to zero at $E_F$ resulting in Mn moments with more local character. However even for the Mn sites the minority-spin gap in CMA is less well defined than in CMS. This would explain the weaker multiplet features in the Mn XMCD from the CMA sample, owing to a reduced localisation of the Mn moment.

Previous authors have suggested that the fine structure in the Co and Mn XMCD is related to the detailed shape of the unoccupied states in the PDOS [refs.]. From these arguments the more metallic looking Co XMCD seen here for the CMA film could be explained in terms of the broader DOS obtained in the B2 structure as opposed to the $L2_1$ structure of CMS films [14,19]. However there are two principal objections to these arguments: (i) calculations of the XMCD based purely on band structure considerations do not accurately reproduce the fine structure in the Co XMCD [19]; and (ii) the PDOS calculated for both Co and Mn unoccupied states are broader for the B2 ordered CMA film than the $L2_1$ CMS film, and yet the width of the main XMCD peaks and fine structure features are comparable for the two Mn XMCD spectra shown in Fig. 2(b).

The XMCD curves obtained around the Co and Mn $L_{2,3}$ absorption edges are compared to atomic multiplet calculations in Fig. 4. Details of the calculational method can be found in ref. [20]. *Some specific details of multiplet calculations to go here {GVL} – also mention sigma used for calc curves in fig 4 {NDT}.* It can be seen from Fig. 4a that the Co XMCD spectrum bears some similarity to the calculated spectra for localised divalent Co atoms. The strong Co-Co and Co-Mn hybridisation leads to a weakening of the multiplet features in the experimental spectra compared to the calculations. This makes direct comparisons difficult, although the calculation using a tetrahedral crystal field appears to give a better match with the data. This is consistent with the expected crystal symmetry in the full Heusler alloy structure where the Co atoms sit in tetrahedral sites with respect to the first neighbour Mn atoms. However the second neighbour Co-Co interactions are also important in the full Heusler alloys, and

this leads to octahedral crystal field splitting [2,3]. The Mn XMCD spectrum (Fig. 4b) shows some of the fine structure produced in the multiplet calculation for Mn with $d^5$ valency, most notably around the $L_2$ absorption edge. However the features around the $L_3$ absorption edge are not well reproduced in the calculation, suggesting an alternative or possibly mixed valence state could occur for Mn in the CMS film.

The XA and XMLD spectra obtained from the CMS film around the Mn $L_{2,3}$ absorption edges are shown in Fig 5, for measurements obtained along the <100> and <110> directions. It can be seen that a reasonably substantial linear dichroism effect is obtained in this sample (~4.5%, taken as the ratio of the maximum XMLD to the $L_3$ absorption peak height). Although the size of the effect is not as large as that observed in localised charge systems, such as diluted $Mn^{2+}$ ions in GaAs [11], it is still several times larger than would be anticipated from a metallic system. Further, the anisotropy in the XMLD that was found in ref. [11], is also clearly evident here as can be seen by the changing spectral shape for measurements along the two sample axes. We also note that, despite differences in the individual XMLD scans obtained here and their counterparts in the previous paper [11], the mean spectra are very similar.

The much larger XMLD feature at the $L_2$ absorption edge seen in Fig. 5 compared to the previous work [11], is due to the greater intensity of the $L_2$ XAS peak in the CMS film compared to a localised charge system (for example a metallic oxide). In fact the relative intensities of the XMLD at the $L_3$ and $L_2$ absorption edges are similar to those seen in metallic systems [21,22]. The corresponding XA and XMLD spectra obtained around the Co $L_{2,3}$ absorption edges of the CMS film are shown in Fig. 6. A strong dichroism effect is also seen at these absorption edges (~6%). This effect is approximately 3 times larger than that seen in pure metallic Co films [21,22]. To our knowledge these are the first observations of an enhanced XMLD in a half-metallic alloy, and indicate a degree of localisation of the Co and Mn moments. Unlike the Mn absorption edges, at the Co edges there is little apparent anisotropy in the linear dichroism, resulting in a nearly vanishing mean XMLD curve.

The XA and XMLD spectra measured at the Mn and Co absorption edges for the CMA sample are shown in Figs. 7 and 8, respectively. Again a strong anisotropy is seen in the Mn XMLD (Fig. 7), although the magnitude of the dichroism is reduced by a factor of ~1.8. For the Co XMLD spectra (Fig. 8), the reduction factor is ~3.6 and a slight difference can be seen between the <100> and <110> directions. By applying a standard sum rule analysis [23] to the measured XMCD spectra, the ratios of the total

Co and Mn atomic moments between the CMS and CMA samples, i.e. the values of ($\mu_{Co}^{CMS}$/ $\mu_{Co}^{CMA}$) and ($\mu_{Mn}^{CMS}$/ $\mu_{Mn}^{CMA}$) were determined to be ~1.52 and ~1.25 respectively. This calculation assumes that the number of 3*d* holes and the degree of Mn *j*=3/2 and *j*=1/2 mixing [10] are the same for both samples. Previous theoretical calculations of these moments [24] give values for these ratios of ~1.34 and ~1.16, which are smaller but in consistent proportions to the values determined here. As the XMLD intensity is proportional to the expectation value of the atomic moment [11,12,21,22], the scaling factor of the XMLD between the CMS and CMA samples, due purely to the measured atomic moment ratios (above) would be ~2 for Co and ~1.5 for Mn. Whilst this accounts for most of the change in the Mn XMLD, it is only about half of the change seen in the Co XMLD. The origin of the remaining reduction in the Co XMLD must therefore be the change in the degree of localisation of the Co moment, as suggested from the XMCD measurements.

Further evidence to support this conclusion can be found by comparing the lineshape of the XMLD (measured along the <100> direction) from the two Heusler samples and a FeCo/GaAs thin film standard sample [25], as shown in Fig. 9. It can be seen that the spectrum from the CMA sample closely resembles that of the metallic FeCo film, whereas the CMS spectrum comprises sharper features. Thus it appears that the Co moments in the CMA film are more metallic in nature than those of the CMS sample. However, as can be seen by comparing Fig. 8 and Fig. 6, the anisotropy in the Co XMLD is greater in the CMA film than the CMS sample. This could be related to the different crystal structures of the Heusler alloys, B2 for CMA and $L2_1$ for the CMS, resulting in different crystal field symmetries. Further to the measurements presented here, it was found that the anisotropy in the Co XMLD was even greater in a CMA sample measured in the as-prepared (and thus least ordered) state. These results will be presented elsewhere. The survival of the crystal field splitting of the empty *d* states depends on the Co-Co and Co-Mn hybridisation which lies at the heart of the formation of the minority-spin gap in the full Heusler alloys. XMLD may therefore offer a unique method for probing subtle changes in the interatomic hybridisation in Heusler alloys, via changes in the crystal field symmetry.

## IV. CONCLUSION

In summary, we have utilised x-ray magnetic circular and linear dichroism measurements around the $L_{2,3}$ absorption edges to probe the localised character of the Co and Mn interface moments in half-metallic Heusler films. A multiplet fine structure was found in the XMCD curves, and an enhanced x-ray magnetic linear dichroism was observed in the $Co_2MnSi$ (CMS) sample, for both Co and Mn absorption edges. Whilst these two characteristics were largely retained at the Mn absorption edges in the $Co_2MnAl$ (CMA) sample, they were both reduced at the Co absorption edges. These measurements suggest that, although the Mn moments in both Heusler alloys show some localised character, the Co moments are less well localised in CMA. The local moment behaviour can be related to the partial density of states (PDOS) within the band gap due to the local exclusion of minority-spin around a given atomic site. For CMA films, the calculated PDOS yields a larger effective minority-spin gap for Mn than for Co states. Thus this result provides crucial experimental validation of the calculated partial density of states (PDOS) and the nature of the minority-spin band gap in these Heusler alloys. As the overall band gap is determined by the Co PDOS, the observation of localised Co moments by the x-ray methods used here should coincide with the onset of half-metallic behaviour. In fact, magnetotransport measurements on these samples yielded a significantly larger spin-polarisation for the CMS film [6] compared to the CMA sample, in agreement with the results presented here.

## Acknowledgements

The Advanced Light Source is supported by the Director, Office of Science, Office of Basic Energy Sciences, of the U.S. Department of Energy under Contract No. DE-AC02-05CH11231. A part of this work was supported by the Grant Program of the New Energy and Industrial Development Organization (NEDO), and by a Research Fellowship for Young Scientists from the Japan Society for the Promotion of Science (JSPS).

1. R. A. de Groot, F. M. Mueller, P. G. van Engen and K. H. J. Buschow, Phys. Rev. Lett. **50**, 2024 (1983).
2. I. Galanakis, P. H. Dederichs, and N. Papanikolaou, Phys. Rev. B **66**, 174429 (2002).
3. I. Galanakis, Ph Mavropoulos and P. H. Dederichs, J. Phys. D: Appl. Phys. **39**, 765 (2006)
4. H. C. Kandpal, G. H. Fecher, and C. Felser, J. Phys. D: Appl. Phys. **40**, 1507 (2007).
5. Y. Sakuraba, J. Nakata, M. Oogane, H. Kubota, Y. Ando, A. Sakuma, and T. Miyazaki, Jpn. J. Appl. Phys. **44**, L1100 (2005).
6. M. Oogane, Y. Sakuraba, J. Nakata, H. Kubota, Y. Ando, A. Sakuma, and T. Miyazaki, J. Phys. D: Appl. Phys. **39**, 834 (2006).
7. Y. Sakuraba, M. Hattori, M. Oogane, Y. Ando, H. Kato, A. Sakuma, H. Kubota and T. Miyazaki, Appl. Phys. Lett. **88**, 192508 (2006).
8. J. Kübler, A. R. Williams and C. B. Sommers, Phys. Rev. B **28**, 1745 (1983).
9. P. Gambardella, S. S. Dhesi, S. Gardonio, C. Grazioli, P. Ohresser, and C. Carbone, Phys. Rev. Lett. **88**, 047202 (2002).
10. K. W. Edmonds, N. R. S. Farley, T. K. Johal, G. van der Laan, R. P. Campion, B. L. Gallagher, and C. T. Foxon, Phys. Rev. B **71**, 064418 (2005).
11. A. A. Freeman, K. W. Edmonds, G. van der Laan, N. R. S. Farley, T. K. Johal, E. Arenholz, R. P. Campion, C. T. Foxon, and B. L. Gallagher, Phys. Rev. B **73**, 233303 (2006).
12. G. van der Laan, E. Arenholz, R. V. Chopdekar and Y. Suzuki, Phys. Rev. B **77**, 064407 (2008); E. Arenholz, G. van der Laan, R. V. Chopdekar and Y. Suzuki, Phys. Rev. Lett **98**, 197201 (2007).

13. E. Arenholz and S. O. Prestemon, Rev. Sci. Instrum. **76**, 083908 (2005).
14. J. Schmalhorst, A. Thomas, S. Kämmerer, O. Schebaum, D. Ebke, M. D. Sacher, G. Reiss, A. Hütten, A. Turchanin, A. Gölzhäuser, and E. Arenholz, Phys. Rev. B **75**, 014403 (2007).
15. N. D. Telling, P. S. Keatley, G. van der Laan, R. J. Hicken, E. Arenholz, Y. Sakuraba, M. Oogane, Y. Ando, and T. Miyazaki, Phys. Rev. B **74**, 224439 (2006).
16. T. Saitoa, T. Katayama, T. Ishikawa, M. Yamamoto, D. Asakura and T. Koide, Appl. Phys. Lett. **91**, 262502 (2007).
17. A. Kimura, S. Suga, T. Shishidou, S. Imada, T. Muro, S. Y. Park, T. Miyahara, T. Kaneko, and T. Kanomata, Phys Rev. B **56**, 6021 (1997).
18. K. Miyamoto, K. Ioria, A. Kimuraa, T. Xiea, M. Taniguchia,b, S. Qiaob, and K. Tsuchiyac, Solid State Comm. **128**, 163 (2003).
19. V. N. Antonova, O. Jepsenb, A. N. Yaresko, A. P. Shpak, J. Appl. Phys. **100**, 043711 (2006).
20. G. van der Laan and B. T. Thole, Phys. Rev. B **43**, 13401 (1991).
21. M. M. Schwickert, G. Y. Guo, M. A. Tomaz, W. L. O'Brien and G. R. Harp, Phys. Rev. B **58**, R4289 (1998).
22. S. S. Dhesi, G. van der Laan, E. Dudzik and A. B. Shick, Phys. Rev. Lett. **87**, 067201 (2001).
23. C. T. Chen, Y. U. Idzerda, H.–J. Lin, N. V. Smith, G. Meigs, E. Chaban, G. H. Ho, E. Pellegrin, and F. Sette, Phys. Rev. Lett. **75**, 152 (1995); B. T. Thole, P. Carra, F. Sette, and G. van der Laan, Phys. Rev. Lett. **68**, 1943 (1992).
24. I. Galanakis, Phys. Rev. B **71**, 012413 (2005).
25. E. Arenholz, Y.U. Idzerda, G. Van der Laan, unpublished

FIG. 1: Schematic showing the various geometries used for XMCD measurements (a) and XMLD measurements, (b) and (c). (color online)

FIG. 2: XMCD measured around (a) the Co $L_{2,3}$ absorption edges and (b) the Mn $L_{2,3}$ absorption edges. In (a) spectra from the $Co_2MnSi$ (CMS) and $Co_2MnAl$ (CMA) film are compared to a Co/Al reference sample. The Mn spectra obtained for CMS (solid black line) and CMA (thin red line) are overlaid in (b). The arrows indicate the positions of multiplet fine structure. (color online).

FIG. 3: The calculated partial density of states (PDOS) for Co, Mn and Al in the $Co_2MnAl$ B2 structure. The inset shows and enlargement around the Fermi level.

FIG. 4: (a) XMCD recorded around the Co $L_{2,3}$ absorption edges for $Co_2MnSi$ (top curve) and multiplet calculations for $d^7$ atomic Co using tetrahedral (Td) and octahedral (Oh) crystal fields. (b) XMCD recorded around the Mn $L_{2,3}$ absorption edges (top curve) and multiplet calculation for Mn in the $d^5$ valence state, assuming spherical symmetry.

FIG. 5: Mn $L_{2,3}$ x-ray absorption (XA) spectra (top) measured for the $Co_2MnSi$ film along the <100> and <110> crystal axes. The red and blue curves correspond to measurements made with the magnetic field applied parallel and orthogonal to linear polarisation vector. The XA spectra were normalised to 1 at the $L_3$ maximum and have been displaced vertically for clarity. The corresponding XMLD spectra obtained by subtraction of the two XA curves for each crystal direction, together with the mean of these spectra, are shown underneath.

FIG. 6: Co $L_{2,3}$ x-ray absorption (XA) spectra (top) measured for the $Co_2MnSi$ film along the <100> and <110> crystal axes. The red and blue curves correspond to measurements made with the magnetic field applied parallel and orthogonal to linear polarisation vector. The XA spectra were normalised to 1 at the $L_3$ maximum and have been displaced vertically for clarity. The corresponding XMLD spectra obtained by subtraction of the two XA curves for each crystal direction, together with the mean of these spectra, are shown underneath.

FIG. 7: As Fig. 5, but for the $Co_2MnAl$ thin film.

FIG. 8: As Fig. 6, but for the $Co_2MnAl$ thin film.

FIG. 9: XMLD at the Co $L_{2,3}$ absorption edges measured along the <100> crystal axes, for the $Co_2MnSi$ and $Co_2MnAl$, compared to a reference sample of FeCo/GaAs. The XMLD was normalised to 1 at the $L_3$ maximum. The curves have been displaced vertically for clarity.

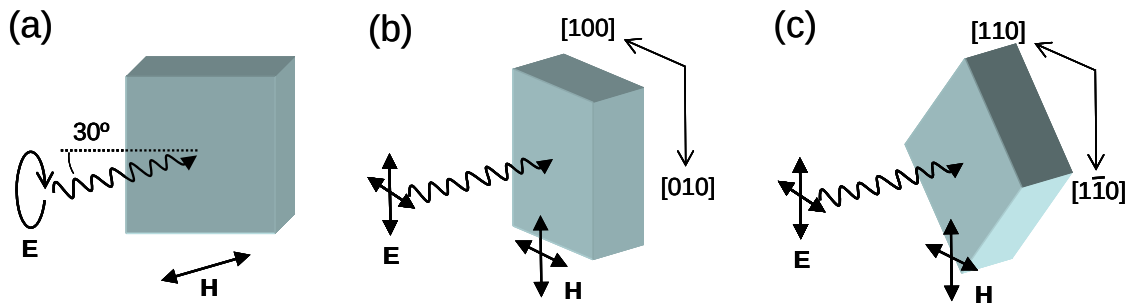


*Figure 1, Telling et al*

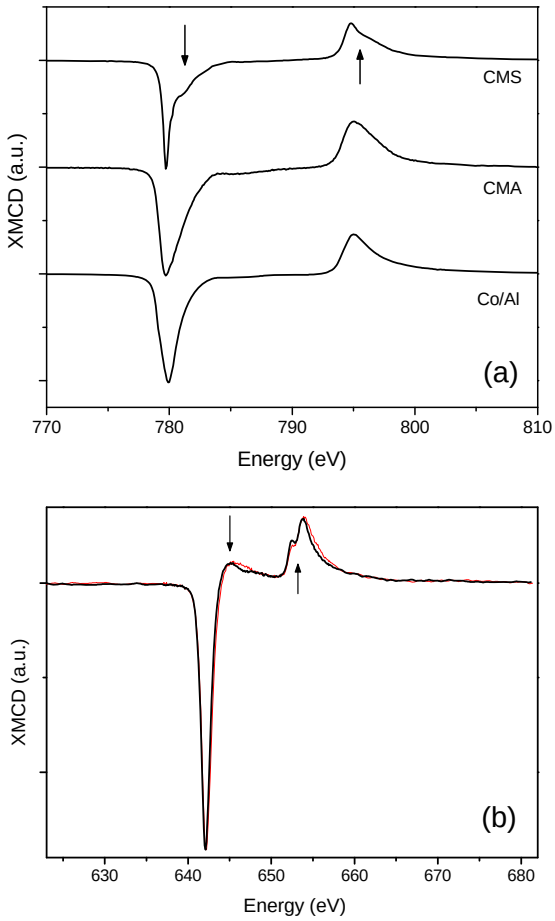


*Figure 2, Telling et al*

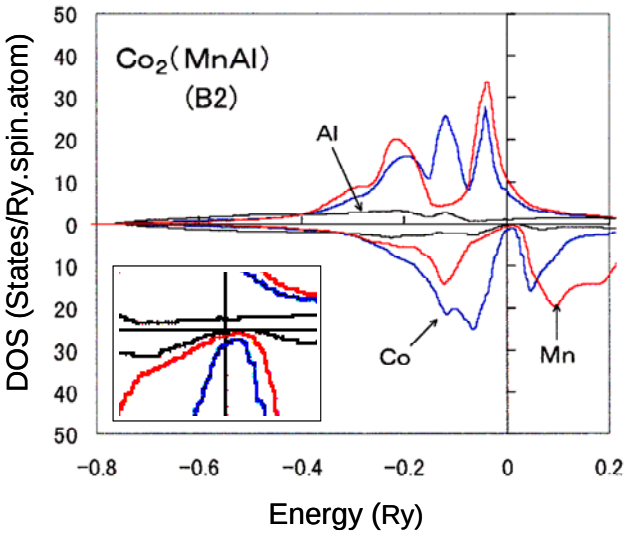


*Figure 3, Telling et al*

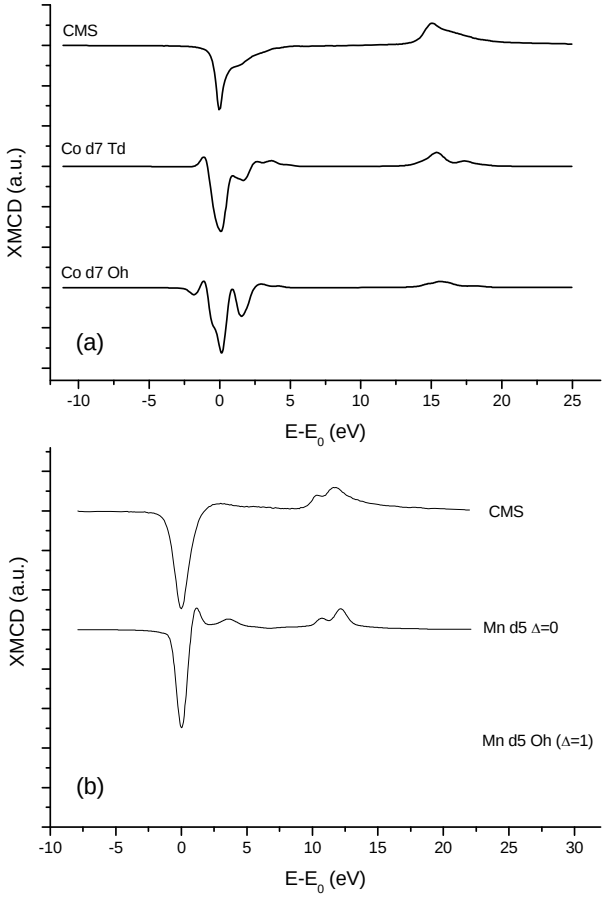


*Figure 4, Telling et al*

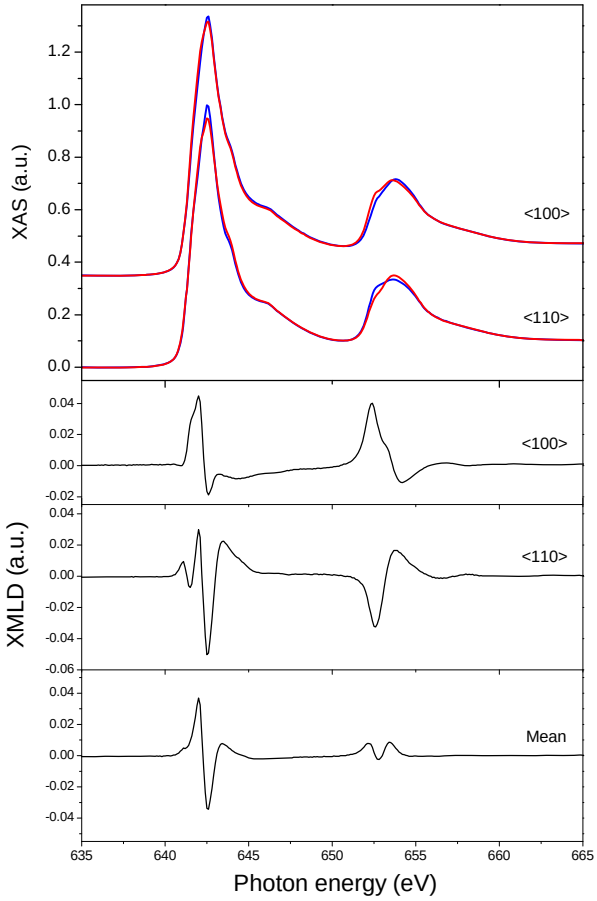


*Figure 5, Telling et al*

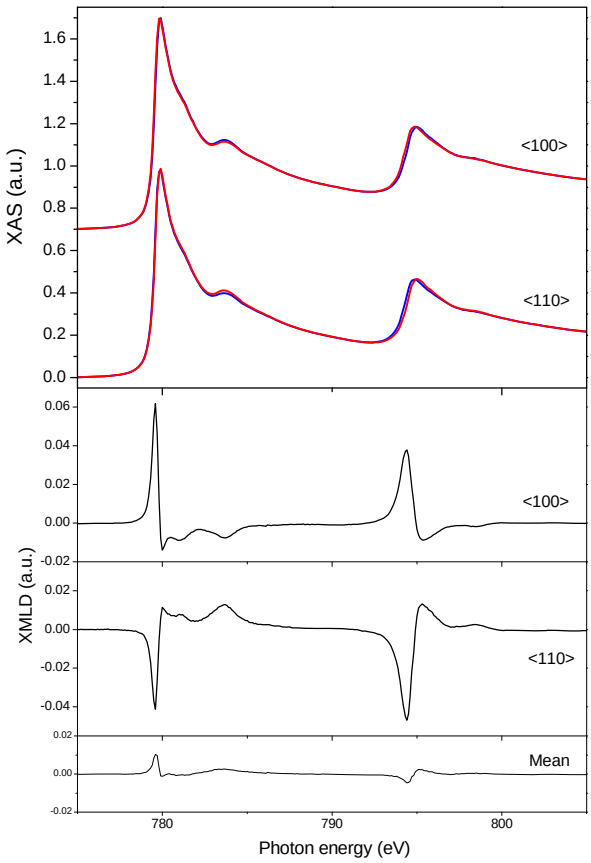


*Figure 6, Telling et al*

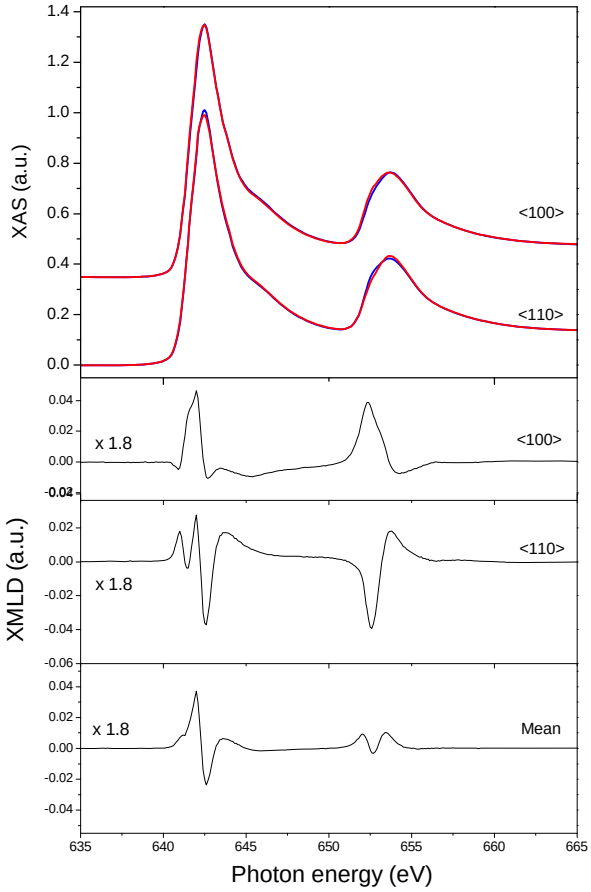


*Figure 7, Telling et al*

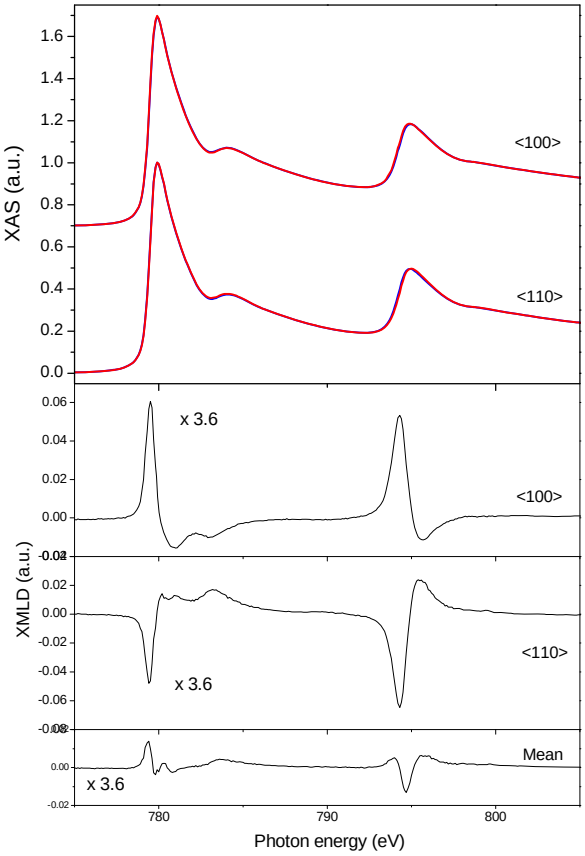


*Figure 8, Telling et al*

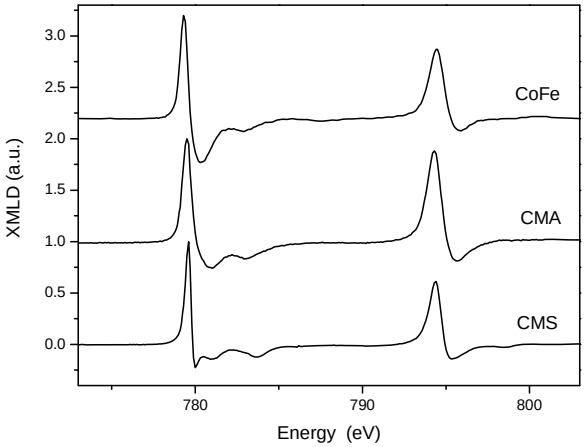


*Figure 9, Telling et al*